This article was downloaded by: *[Zhang, XinFeng]*
On: *6 October 2010*
Access details: *Access Details: [subscription number 927357366]*
Publisher *Taylor & Francis*
Informa Ltd Registered in England and Wales Registered Number: 1072954 Registered office: Mortimer House, 37-41 Mortimer Street, London W1T 3JH, UK

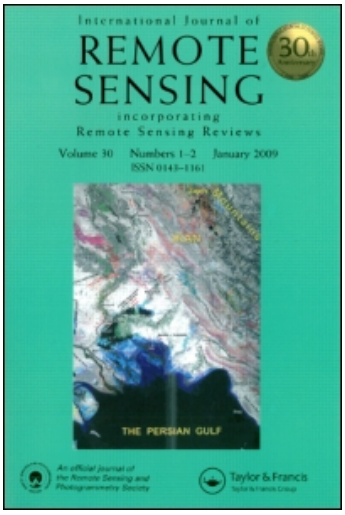

International Journal of Remote Sensing
Publication details, including instructions for authors and subscription information:
http://www.informaworld.com/smpp/title~content=t713722504

Analysis of the spatio-temporal distribution of chlorophyll-*a* in the eastern Indian Ocean near the time of the 2004 South Asian tsunami

Xinfeng Zhang[a]; Danling Tang[b]; Zizhen Li[c]; Zhongzheng Yan[b]; Fengpan Zhang[d]
[a] College of Marine Sciences, Key Laboratory of Sustainable Exploitation of Oceanic Fisheries Resources under Ministry of Education, Shanghai Ocean University, Lingang Xincheng, Shanghai, China [b] Center of Remote Sensing on Marine Ecology/Environment (RSMEE), LED, South China Sea Institute of Oceanology, Chinese Academy of Sciences, Guangzhou, China [c] Institute of Bioinformatics, School of Mathematics and Statistics, Lanzhou University, Lanzhou, China [d] School of Mathematics and Information Sciences, Henan University, Kaifeng, China

Online publication date: 28 September 2010

To cite this Article Zhang, Xinfeng , Tang, Danling , Li, Zizhen , Yan, Zhongzheng and Zhang, Fengpan(2010) 'Analysis of the spatio-temporal distribution of chlorophyll-*a* in the eastern Indian Ocean near the time of the 2004 South Asian tsunami', International Journal of Remote Sensing, 31: 17, 4579 — 4593
To link to this Article: DOI: 10.1080/01431161.2010.485141
URL: http://dx.doi.org/10.1080/01431161.2010.485141

PLEASE SCROLL DOWN FOR ARTICLE

Full terms and conditions of use: http://www.informaworld.com/terms-and-conditions-of-access.pdf

This article may be used for research, teaching and private study purposes. Any substantial or systematic reproduction, re-distribution, re-selling, loan or sub-licensing, systematic supply or distribution in any form to anyone is expressly forbidden.

The publisher does not give any warranty express or implied or make any representation that the contents will be complete or accurate or up to date. The accuracy of any instructions, formulae and drug doses should be independently verified with primary sources. The publisher shall not be liable for any loss, actions, claims, proceedings, demand or costs or damages whatsoever or howsoever caused arising directly or indirectly in connection with or arising out of the use of this material.

International Journal of Remote Sensing
Vol. 31, Nos. 17–18, September 2010, 4579–4593

Taylor & Francis
Taylor & Francis Group

Analysis of the spatio-temporal distribution of chlorophyll-*a* in the eastern Indian Ocean near the time of the 2004 South Asian tsunami

XINFENG ZHANG†, DANLING TANG*‡, ZIZHEN LI§, ZHONGZHENG YAN‡ and FENGPAN ZHANG¶

†College of Marine Sciences, Key Laboratory of Sustainable Exploitation of Oceanic Fisheries Resources under Ministry of Education, Shanghai Ocean University, Lingang Xincheng, Shanghai, 201306 China

‡Center of Remote Sensing on Marine Ecology/Environment (RSMEE), LED, South China Sea Institute of Oceanology, Chinese Academy of Sciences, Guangzhou, 510301 China

§Institute of Bioinformatics, School of Mathematics and Statistics, Lanzhou University, Lanzhou, 730000 China

¶School of Mathematics and Information Sciences, Henan University, Kaifeng, 475001 China

Downloaded By: [Zhang, XinFeng] At: 12:35 6 October 2010

This study analysed the spatio-temporal distributions of chlorophyll-*a* (chl-*a*) in the Indian Ocean during the 2004 South Asian tsunami and the effects of four variables (sea surface temperature, normalized water-leaving radiance, rainfall and wind speed) on chl-*a* distributions during the tsunami, using satellite data and spatial models. The results showed considerable variations in the spatio-temporal distributions of chl-*a*, and the effects of the four variables on chl-*a* around the tsunami. The results revealed that sea surface temperature and rainfall had negative effects on chl-*a*, while normalized water-leaving radiance and wind speed had positive effects. The effects of all the four explanatory variables were significant (positive or negative) before the tsunami. Except normalized water-leaving radiance, the other three variables all showed certain degrees of weakened effects on chl-*a* after the tsunami, which suggested the physical disturbance of the tsunami on the effects of these variables on chl-*a* distribution.

1. Introduction

The $M_w = 9.3$ earthquake, centred off the west coast of northern Sumatra (3.316°N, 95.854°E) on 26 December 2004, produced the largest trans-oceanic tsunami ever recorded (Stein and Okal 2005). This tsunami was an unprecedented natural disaster that caused massive damage to the marine and terrestrial ecosystems and the environment along the coastal area (Liu *et al*. 2005, UNEP 2005). The physical disturbance is an important factor structuring marine ecosystems (Sousa 1979, Krishnakutty 2006, Tang *et al*. 2009) and will have a long-lasting impact on the biotic communities and their habitats.

Earthquakes can induce sudden changes in ocean–atmosphere interactions and the consequences of these – the anomalous behaviour of numerous oceanic and atmospheric processes – are believed to show precursory signals (Dey and Singh 2003, Dey *et al*. 2004). One such process is the change in distribution of chlorophyll-*a* (chl-*a*) on the ocean surface (Tang *et al*. 2006c). Chl-*a* results from the growth of phytoplankton

*Corresponding author. Email: lingzistdl@126.com

International Journal of Remote Sensing
ISSN 0143-1161 print/ISSN 1366-5901 online © 2010 Taylor & Francis
http://www.tandf.co.uk/journals
DOI: 10.1080/01431161.2010.485141

and is an indicator of primary productivity in marine ecosystems. The spatial and temporal distribution of chl-*a* is correlated closely with many oceanic and atmospheric factors, e.g. sea surface temperature (SST), spatial location (offshore distance), wind (velocity and direction), rainfall, suspended sediment concentration and nutrients (Tang *et al*. 2004, 2006a, 2006b). Tang *et al*. (2006c) first investigated the effect of the South Asian tsunami on marine phytoplankton in the Indian Ocean. They found an increase in the chl-*a* level along the east coast of India and around Sri Lanka, prior to the tsunami, and a chl-*a* bloom spread afterwards along the drift of the current. They also revealed an inverse relationship between chl-*a* and SST.

Other studies on the effect of the 2004 tsunami include using satellite data to investigate the changes in SST and chl-*a*. Singh *et al*. (2007) found anomalous changes in SST before and after the earthquake. By studying SST and the integrated water vapour following the event on 26 December 2004, Agarwal *et al*. (2007) found that the overall air–sea interaction underwent a change but recovered slowly to its normal behaviour afterwards. Changes in suspended sediments in the eastern Indian Ocean associated with the 2004 tsunami were also observed (Yan and Tang 2008). By comparing Modis Aqua satellite images, Tan *et al*. (2007) concluded that chl-*a* at the upwelling area at the northern Malacca Straits did not exhibit any significant changes in relation to tsunami waves. Modelling the satellite Sea-viewing Wide Field-of-view Sensor (SeaWiFS) data indicated that the effects of wind speed and rainfall on suspended sediment concentration weakened immediately around the tsunami event (Zhang *et al*. 2009).

These studies have significantly advanced our understanding of the effect of tsunami on chl-*a* and SST. A question that remains to be explored is how chl-*a* was distributed before and after the tsunami and what factors in addition to SST would have affected its distribution. In this study, we used satellite data before and after the tsunami to model the spatial and temporal dynamics of chl-*a* in terms of SST, normalized water-leaving radiance (NWR), wind speed (WIN) and rainfall (RAF). An important feature of our models is that it accounts for the spatial autocorrelation in the distribution of chl-*a*. Our objectives are to find out whether the spatial distribution of chl-*a*, in the severe tsunami-affected ocean surface area, remained the same before and after the tsunami, and what oceanic and atmospheric factors affected the dynamics in chl-*a*.

Downloaded By: [Zhang, XinFeng] At: 12:35 6 October 2010

2. Study area and materials

2.1 *Study area*

The study area is located at 5°S–11°N, 74–98°E in the eastern Indian Ocean (figure 1(*a*) box E), which covers the earthquake epicentre and was influenced most strongly by the tsunami. The study area (excluding land) is subdivided into 1528 grids (with resolution $0.5^\circ \times 0.5^\circ$).

2.2 *Satellite data*

Data in seven temporal periods (conveniently called 'week' hereafter) were obtained (table 1). Three 'weeks' occurred before the week of the tsunami and three after. Each 'week' has eight days, except the tsunami week (26–31 December, week 4), which was arbitrarily determined by the satellite. For comparison of the chl-*a* distribution

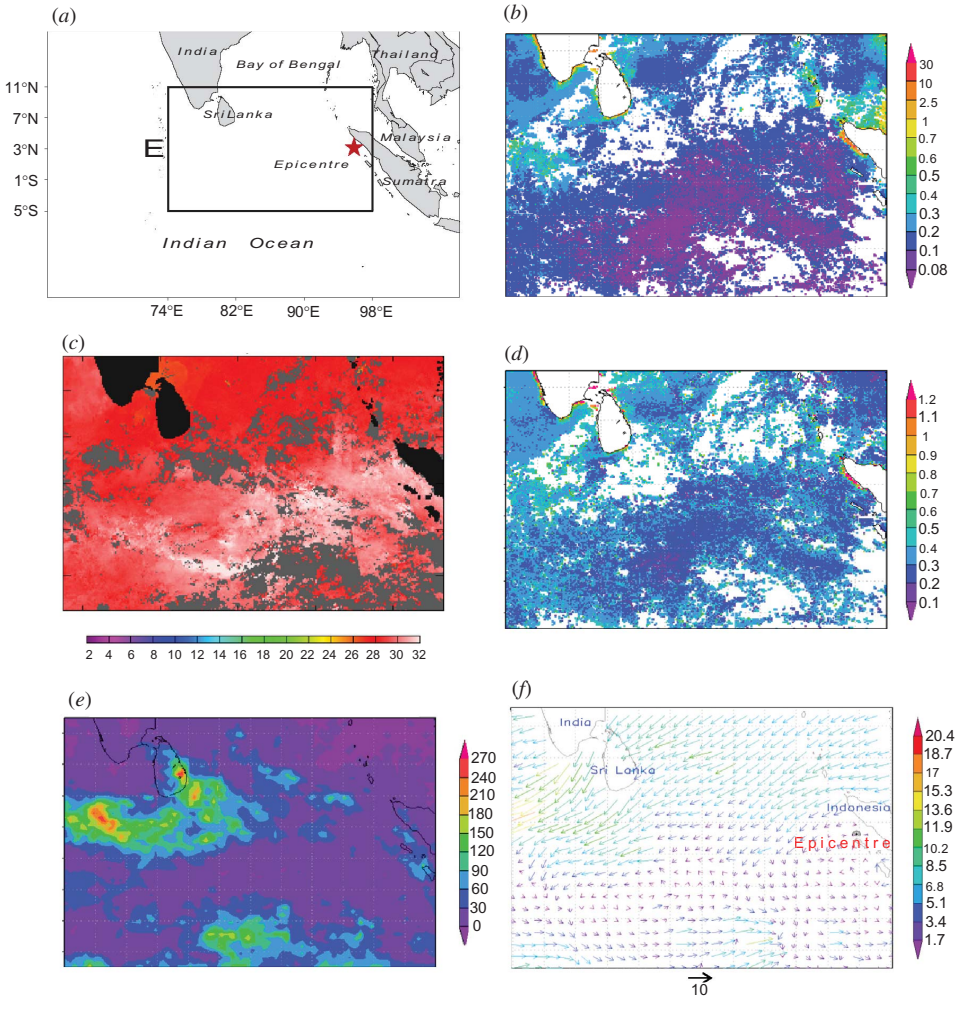

Figure 1. (*a*) Box E shows the study area (5°S–11°N, 74–98°E). The epicentre is marked with a red star. (*b*)–(*f*) Distributions of chl-*a* (mg m^{-3}), SST (°C), NWR (mW cm^{-2} μm^{-1} sr^{-1}), RAF (mm) and WIN (m s^{-1}) in the study area in the tsunami week (26–31 December 2004), respectively.

Table 1. The first-order spatial autocorrelation in chl-*a* among the adjacent neighbours as measured by Moran's *I*.

Date (Week)	2–9 December 2004 (1)	10–17 December (2)	18–25 December (3)	26–31 December (4)	1–8 January 2005 (5)	9–16 January (6)	17–24 January (7)
Moran's *I* (chl-*a*)	0.65	0.74	0.62	0.70	0.59	0.75	0.71

The correlations are highly significant, with *P*-value for each *I* smaller than 0.0001. Week 4 is the tsunami week.

Downloaded By: [Zhang, XinFeng] At: 12:35 6 October 2010

between the tsunami and non-tsunami periods, another six weeks of data (three before the seven-week tsunami period and three after) were analysed later.

The chl-*a* and NWR data, observed from SeaWiFS, at 0.5° resolution and at 555 nm eight-day (level 3), were obtained from the Ocean Color Time Series Project (http://reason.gsfc.nasa.gov/Giovanni/). Accumulated eight-day RAF data, at 0.5° resolution and observed from the satellite (Daily) Tropical Rainfall Measuring Mission (TRMM) (3B42 V6), were obtained via TRMM Online Visualization and Analysis System (TOVAS; http://disc2.nascom.nasa.gov/Giovanni/tovas/). Eight-day SST data (level 3), at 9 km resolution, were collected by the satellite Moderate Resolution Imaging Spectroradiometer (MODIS) (Aqua). Wind vector daily data (level 3), at 0.25° resolution, were observed from satellite QuickScat. SST and wind vector data were obtained from the Jet Propulsion Laboratory (http://poet.jpl.nasa.-gov/). Level-3 data used in this study are high-level data of research quality. In order to analyse the data at the same scale, we aggregated the 9 km resolution SST data up to 0.5° resolution. We averaged wind vector data for each of the seven weeks, from 2 December 2004 to 24 January 2005, along longitude and latitude directions. We then aggregated the wind vector from 0.25° to 0.5° resolution.

Before modelling chl-*a* in relation to the four explanatory variables (SST, NWR, RAF and WIN), an exploratory data analysis was undertaken to ensure the quality of the data. A very small portion of 'outliers' in chl-*a*, NWR, RAF, SST and WIN were identified. These data were excluded in the modelling. We also omitted those locations where data are missing.

Downloaded By: [Zhang, XinFeng] At: 12:35 6 October 2010

3. Models and methods

Due to the flow of sea water or other reasons, the values of chl-*a* at two neighbouring locations (or grids) are not independent but tend to be similar, i.e. the values of chl-*a* at neighbouring locations are positively correlated. The spatial autocorrelation makes the ordinary regression methods invalid. To overcome the problem, we applied the spatial autoregressive models that are often used in spatial statistics (Anselin 1988). Spatial models, accounting for the effect of autocorrelation, are widely used in geographical research (Griffith 1987, Odland 1987), spatial econometrics (Anselin 1988, Anselin and Florax 1995), public health (Waller and Gotway 2004) and ecology (Borcadrd and Legendre 2002, Keitt *et al*. 2002).

3.1 *Measuring spatial autocorrelation of chl-a*

A commonly used spatial autocorrelation statistic is Moran's *I*, defined as:

$$I = \boldsymbol{z}'\mathbf{W}\boldsymbol{z}/\boldsymbol{z}'\boldsymbol{z}, \tag{1}$$

where $\boldsymbol{z}$ is $n \times 1$ vector. It is expressed as deviations from the mean, i.e. $z_i = y_i - \bar{y}$, $i = 1 \ldots n$, where y_i is the chl-*a* value at the i^{th} location (or grid). $\boldsymbol{z}'$ is the transpose of $\boldsymbol{z}$ and $\mathbf{W}$ is $n \times n$ spatial weight matrix determined by the spatial configuration of the n locations as:

$$W_{ij} = C_{ij} \Big/ \sum_{j=1}^{j=n} C_{ij} \quad i,j = 1 \ldots n, \tag{2}$$

where $C_{ij} = 1$ if locations i and j are immediate vertical and horizontal neighbours and 0 otherwise. The matrix $(C_{ij})_{n\times n} = C$ is also called a connectivity (or

configuration) matrix (Griffith 1987). Spatial weight matrix **W**, calculated by equation (2), is called row-standardized.

Moran's *I* shows an asymptotic normal distribution (Cliff and Ord 1981). It has an expected value of –[1/(*n* – 1)]. It is close to zero for large *n*. If the values of chl-*a* are independent among spatial locations, the calculated value of *I* should equal this expectation. *I* varies between −1 and +1; the closer the values are to ±1, the stronger are the spatial autocorrelations. Values of *I* that exceed –[1/(*n* – 1)] indicate positive spatial autocorrelation in which neighbouring values tend to be similar. Values below the expectation indicate negative spatial autocorrelation in which neighbouring values tend to be dissimilar.

3.2 *Spatial models*

The general spatial process model is (Anselin 1988):

$$\begin{aligned} \mathbf{y} &= \rho W_1 \mathbf{y} + \mathbf{X}\boldsymbol{\beta} + \boldsymbol{\varepsilon} \\ \boldsymbol{\varepsilon} &= \lambda W_2 \boldsymbol{\varepsilon} + \boldsymbol{\mu} \end{aligned} \quad \boldsymbol{\mu} \sim N\left(0, \sigma^2 I_n\right), \tag{3}$$

where **y** is dependent variable (chl-*a*), ρ is the coefficient of spatially lagged dependent variable $W_1\mathbf{y}$, and λ is the coefficient in spatial autoregressive structure for the error term. W_1 and W_2 are $n \times n$ spatial weight matrices, associated respectively with a spatial autoregressive process in dependent variable **y** and in error term $\boldsymbol{\varepsilon}$. $\boldsymbol{\beta}$ is $k \times 1$ vector of parameters associated with explanatory variables **X** ($n \times k$ matrix). In this study, $k = 4$ is the number of explanatory variables. The noise $\boldsymbol{\mu}$ is normally distributed.

For $\rho = 0$, $\lambda = 0$, model (3) becomes an ordinary linear regression model (OLM), with no spatial effects:

$$\mathbf{y} = \mathbf{X}\boldsymbol{\beta} + \boldsymbol{\varepsilon}. \tag{4}$$

For $\lambda = 0$, the model becomes a mixed regressive-spatial autoregressive model:

$$\mathbf{y} = \rho W_1 \mathbf{y} + \mathbf{X}\boldsymbol{\beta} + \boldsymbol{\varepsilon} \tag{5}$$

Because of the component of spatially lagged variable $W_1\mathbf{y}$, this model is called a spatial lag model (SLM).

For $\rho = 0$, model (3) becomes a mixed regressive-spatial autoregressive model with a spatially autocorrelated error term ε.

$$\begin{aligned} \mathbf{y} &= \mathbf{X}\beta + \boldsymbol{\varepsilon} \\ \boldsymbol{\varepsilon} &= \lambda W_2 \boldsymbol{\varepsilon} + \boldsymbol{\mu}. \end{aligned} \tag{6}$$

Because the spatial dependence is related to error term $\boldsymbol{\varepsilon}$, it is called a spatial error model (SEM).

The properties of the tests (introduced in the next section) are sensitive to the choice of the spatial weight matrix (Anselin and Rey 1991). It is often more convenient in practice to assume the spatial weight matrices W, W_1 and W_2 to be the same (Anselin *et al.* 1996). In this study, the spatial weight matrices W, W_1 and W_2 were all determined and calculated by equation (2). Alternatively, higher-order configurations and distance-weighted matrices may be used (Anselin 1988).

Downloaded By: [Zhang, XinFeng] At: 12:35 6 October 2010

3.3 *Estimation methods*

In order to understand the tsunami influence on chl-*a*, we first used Moran's *I* to examine the spatial autocorrelation in chl-*a* and its possible temporal change before and after the tsunami. We then modelled chl-*a* (**y**) in relation to the explanatory variables **X** = [SST, NWR, log (RAF+1), WIN], using the models progressively introduced earlier, from OLM, SLM to SEM. Based on an exploratory data analysis, the logarithm of RAF was identified to have a linear relationship with chl-*a*, thus, log(RAF+1) was used to avoid zeroes in the log.

In autoregressive model (3), W_1chl-*a* is just like an explanatory variable. Although the SeaWiFS retrieval of chlorophyll-*a* includes NWR (555) as an input, in order to investigate the mixed effects of NWR and other variables on chl-*a*, NWR could be also used as an explanatory variable.

Normal approximation was used to test the significance of Moran's *I* values for chl-*a*. For model SLM (5), it is well known that the ordinary least squares estimator (OLS) is biased as the observations of chl-*a* are not independent. For model SEM (6), OLS is unbiased but inefficient due to the effects of spatial autocorrelation in the residuals (Anselin 1988).

For general spatial process model (3), we can use the maximum likelihood approach (ML) to estimate the parameters. The unknown parameters are: $\boldsymbol{\theta} = [\rho, \beta, \lambda, \sigma^2]$, the log-likelihood function is obtained as:

$$L(\boldsymbol{\theta}) = -(n/2)\log\pi - (n/2)\log\sigma^2 + \log|B| + \log|A| - \mathbf{v}'\mathbf{v}/2\sigma^2, \tag{7}$$

where $A = I - \rho W_1$, $B = I - \lambda W_2$, $\mathbf{v}'\mathbf{v} = (A\mathbf{y} - \mathbf{X}\beta)'B'B(A\mathbf{y} - \mathbf{X}\beta)$ and $|I - \rho W_1| > 0$, $|I - \lambda W_2| > 0$.

In order to decide which regression model, among the three (OLM, SLM and SEM), is the best choice, we first tested Moran's *I* values of the residuals in OLM. Moran's *I* is useful for indicating the presence of spatial dependence. But it cannot be used to discriminate SLM and SEM if both models have effectively modelled autocorrelation. The Lagrange multiplier tests (LM) are the most appropriate for solving this problem (Anselin and Rey 1991). The LM test is asymptotically distributed as χ^2_q; q is the number of degrees of freedom. LM has four statistics: LMlag, LMerr, RLMlag and RLMerr. Each of the statistics has a complicated mathematical form that is not given here; we refer readers to Anselin *et al.* (1996) for details. Our notation follows the R package 'spdep' (http://www.r-project.org), which was used here for estimating the above models, but it is slightly different from the notation of Anselin *et al.* (1996) with LMlag as their LM_ϕ, LMerr as LM_ψ, RLMlag as LM_ϕ* and RLMerr as LM_ψ*. The LM tests are described as follows. It is clear from the description that RLMlag and RLMerr are the robust versions of LMlag and LMerr, respectively.

1. LMlag is used to test the spatial lag dependence in the absence of spatial error dependence ($\lambda = 0$) under the null hypothesis H_0: $\rho = 0$.
2. RLMlag is used to test the spatial lag dependence in the possible presence of spatial error dependence ($\lambda = 0$ or $\lambda \neq 0$) under the null hypothesis H_0: $\rho = 0$.
3. LMerr is used to test the spatial error dependence in the absence of spatial lag dependence ($\rho = 0$) under the null hypothesis H_0: $\lambda = 0$.
4. RLMerr is used to test the spatial error dependence in the possible presence of spatial lag dependence ($\rho = 0$ or $\rho \neq 0$) under the null hypothesis H_0: $\lambda = 0$.

Downloaded By: [Zhang, XinFeng] At: 12:35 6 October 2010

The decision rule (Anselin and Florax 1995, Anselin *et al*. 1996) is as follows.

1. If both LMlag and LMerr tests are not significant, the OLM model is the final choice.
2. If LMlag is significant (leading to the rejection of H_0: $\rho = 0$) but LMerr is not, the SLM is the proper model and is estimated by RLMlag.
3. If LMerr is significant (leading to the rejection of H_0: $\lambda = 0$) while LMlag is not, then SEM is the better model and is estimated by RLMerr.
4. In the case when both LMlag and LMerr are significant, if LMlag is more significant than LMerr, SLM is taken as the final model and is estimated by RLMlag; while, if LMerr is more significant than LMlag, then SEM is the final choice and is estimated by RLMerr.

We then used the Wald test to test for the significance of parameters in the above models. The Wald statistic is also asymptotically distributed as χ^2_q. All the above computations and model estimations were implemented using the statistical software **R**.

Downloaded By: [Zhang, XinFeng] At: 12:35 6 October 2010

4. Results

Visual inspection on the distributions of chl-*a*, SST, NWR, RAF and WIN for the tsunami week (figure 1(*b*)–(*f*) reveals a possible correlation between SST, NWR and chl-*a*. There is strong positive autocorrelation in the spatial distribution of chl-*a* among neighbouring locations, and the level of correlation remains consistent before and after the tsunami, as indicated by the high values of Moran's *I* (table 1). The high-order spatial correlograms of chl-*a* are shown in figure 2. The autocorrelation decreases gradually as spatial lags increase for all seven weeks. The distance of positive correlation varies considerably among the weeks from 12 lags in Week 5 to 44 lags in Week 2. There is a noticeable wavy shape in the correlogram for the tsunami week (Week 4) and Week 2. This kind of fluctuation was not observed in another six non-tsunami weeks (figure 3). We suggest that these variations are either caused by the tsunami waves or may be an incipient signal of the tsunami. The correlograms in Weeks 1, 6 and 7 in figure 2 are very similar to that in figure 3 and decrease consistently. They are considered to be the 'normal' correlograms with little effect from the tsunami.

The temporal correlation in chl-*a* among the seven weeks is measured by Pearson's product-moment correlation. The results show a strong correlation in chl-*a* between any two weeks (table 2). Although there is a general trend of decrease in correlation over time (along each row of table 2), this pattern is not consistent. The largest correlation coefficient of 0.71 occurred between the tsunami week (Week 4) and Week 6, while the smallest correlation of 0.39 occurred between Weeks 3 and 7.

From the comparison of the overall goodness-of-fit of the three regression models (OLM, SLM and SEM) (table 3), it is evident that the values of Moran's *I* quickly decrease from OLM to SLM to SEM. The very high values (between 0.36 and 0.62) of Moran's *I* for OLM's residuals indicate a high spatial autocorrelation in OLM residuals. Moran's *I* for the SEM residuals are much smaller (between –0.003 and –0.17). Although the significance tests show that Moran's *I* for some of the weeks still differs significantly from zero, the comparison of the correlograms between figures 2 and 4 indicates that the SEM model has effectively captured the spatial structure of chl-*a* distribution. This result is also verified by the Lagrange multiplier test (table 3).

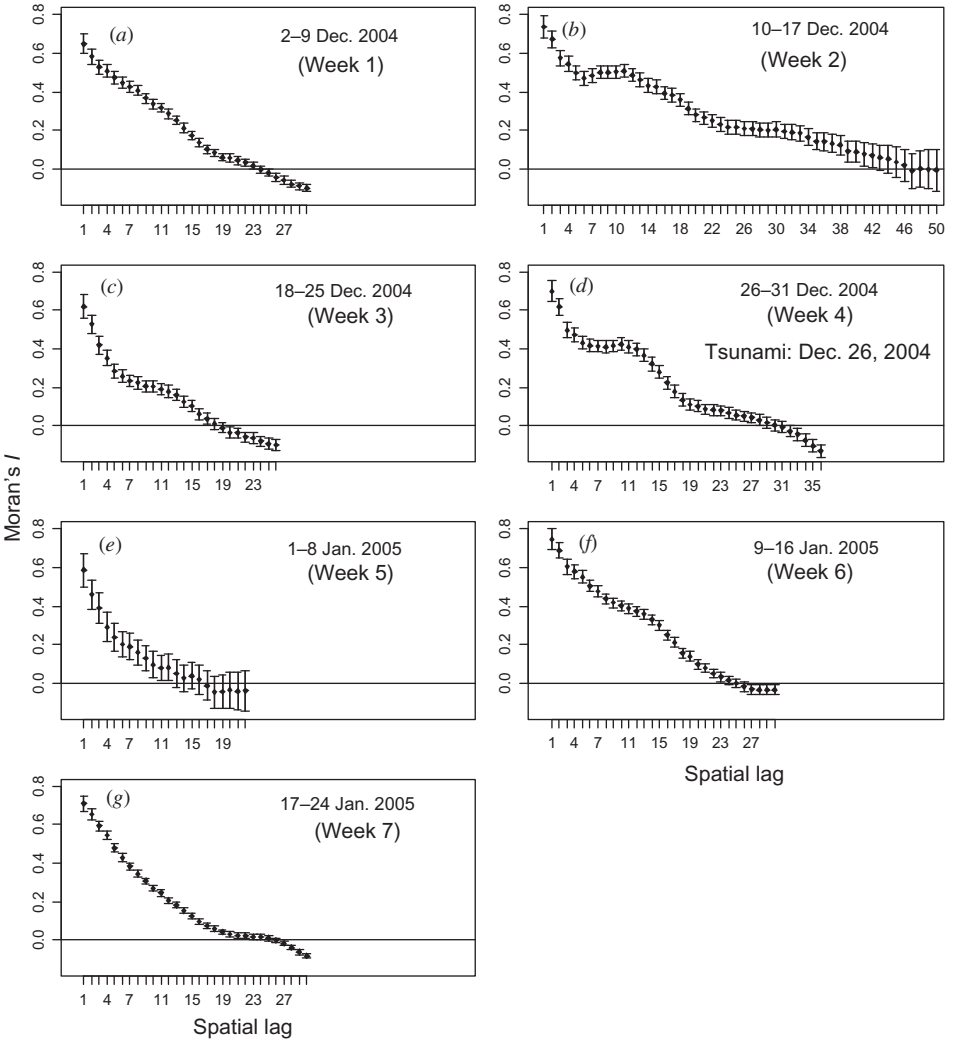

Figure 2. Spatial correlograms for chl-*a* along spatial lag. One spatial lag is 0.5°. The *x*-axis is the number of spatial lags; the *y*-axis is the Moran's *I* value of chl-*a*.

According to the decision rule described in Section 3.3, both LMlag and LMerr are highly significant for every week (table 3). We then went on to estimate the SLM and SEM models with RLMlag and RLMerr, respectively. Results show that RLMerr is highly significant for every week, while RLMlag has much larger *P*-values. This indicates the SEM model is the best for modelling chl-*a* in relation to the four explanatory variables. We then use the SEM to model the distribution of chl-*a* and analyse the temporal effects of the four covariates on chl-*a*.

SST showed a significantly negative correlation with chl-*a*, except in Week 5, immediately after the tsunami week (table 4). The mean value of SST reached the minimum in Week 5 (figure 5). NWR and chl-*a* were always significantly and positively correlated both before and after the tsunami. Except in Week 7, RAF had a strong negative effect on chl-*a* (table 4); RAF reached a minimum value in Week 7

Downloaded By: [Zhang, XinFeng] At: 12:35 6 October 2010

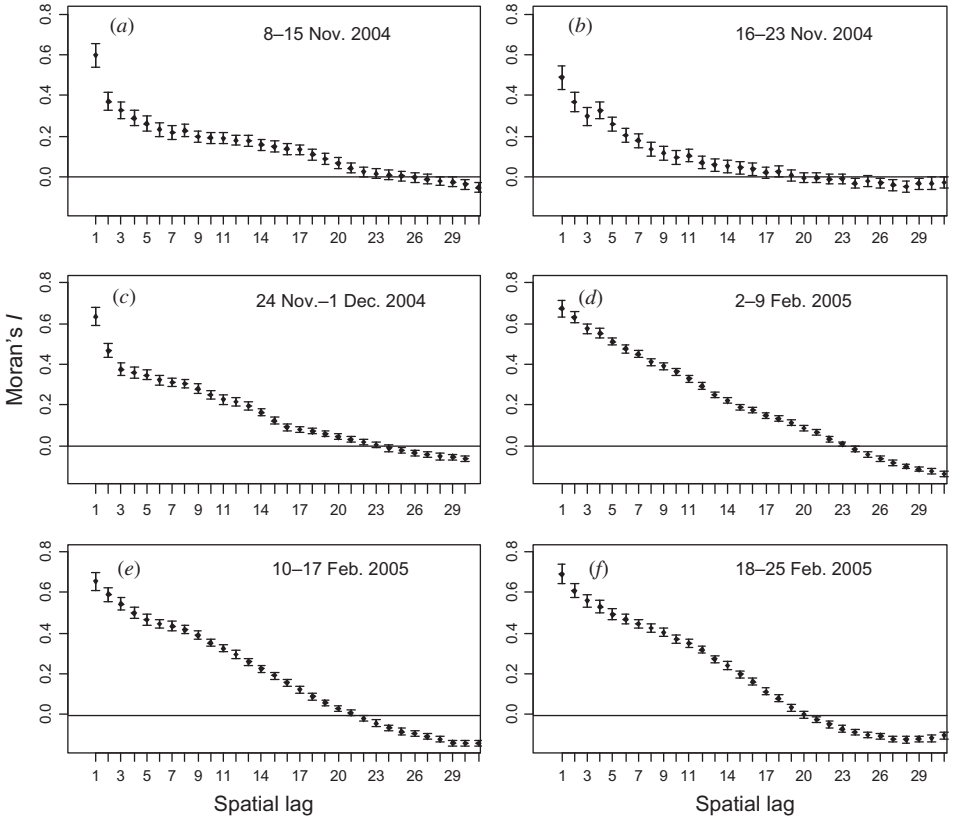

Figure 3. Spatial correlograms for chl-*a* along spatial lag: three weeks before and three weeks after the seven weeks shown in figure 2. The *x*-axis is the number of spatial lags; the *y*-axis is the Moran's *I* value of chl-*a*.

Downloaded By: [Zhang, XinFeng] At: 12:35 6 October 2010

Table 2. Pearson's product-moment correlation coefficient of chl-*a* between weeks.

chl-*a*	Week 2	Week 3	Week 4	Week 5	Week 6	Week 7
Week 1	0.69	0.50	0.59	0.51	0.64	0.50
Week 2		0.68	0.69	0.63	0.68	0.60
Week 3			0.61	0.52	0.63	0.39
Week 4				0.65	0.71	0.55
Week 5					0.67	0.49
Week 6						0.69

P-values for all the correlation coefficients are smaller than 0.001. Weeks 1, 2 . . . 7 are in the order of the seven weeks shown in table 1. Week 4 is the tsunami week.

(figure 5). WIN had a very strong positive influence on chl-*a* before the tsunami. However, this influence decreased dramatically after the tsunami (table 4). WIN did not show an effect on chl-*a* for the two weeks (Weeks 5, 6) immediately after the tsunami week.

Table 3. Tests for the goodness-of-fit of the ordinary linear model (OLM) and the two spatial autoregressive models (SLM and SEM).

Week	1	2	3	4	5	6	7
I for OLM residual	0.51	0.62	0.53	0.55	0.36	0.59	0.59
I for SLM residual	0.07*	0.10	0.06*	0.15	0.14*	0.13	0.03**
I for SEM residual	–0.08*	–0.13	–0.08*	–0.07*	–0.003**	–0.17	–0.11
Lagrange multiplier test to compare SLM and SEM models							
LMerr	419.72	518.33	338.38	409.05	81.89	505.48	805.16
LMlag	344.23	386.74	299.01	300.74	60.19	348.19	713.29
RLMerr	78.13	135.30	48.81	111.82	25.14	165.18	110.41
RLMlag	2.64**	3.70**	9.45*	3.51**	3.45**	7.89*	18.54

*$0.001 < P$-value < 0.05.
**P-value > 0.05.
P-value < 0.001 for others (no asterisk). Weeks 1, 2 . . . 7 are in the order of the seven weeks shown in table 1.

Downloaded By: [Zhang, XinFeng] At: 12:35 6 October 2010

5. Discussion

As a measure of phytoplankton biomass, chl-*a* concentration is important for indicating the changing conditions in the marine ecosystem. Chlorophyll-*a* values derived from ocean colour sensors have been used as a relative measure of phytoplankton abundance and biomass in the ocean (Martin 2004).

5.1 *Spatio-temporal distributions of chl*-a

Results indicate a significant spatio-temporal autocorrelation in chl-*a* during the tsunami period (tables 1 and 2, figure 2). It is obvious that the spatial correlation gradually decreases as spatial lags increase (figure 2), while the attenuation of temporal correlation is smaller (table 2). There is some evidence of fluctuation (or 'anomalous' behaviour) in the spatial correlation in the weeks around the tsunami (figure 2), particularly in Week 2. The wavy correlograms disappeared after the tsunami week. This kind of fluctuation was not found in the other six non-tsunami weeks (figure 3). These abnormal fluctuations should be related to the tsunami event. The significant increase in spatial correlation distance in chl-*a* distribution (figure 2(*b*)), before the tsunami event, indicated that the flow of sea water among neighbouring locations (or grids) was enhanced markedly. Further study is needed to confirm if this phenomenon is a precursory signal of the occurrence of a tsunami.

5.2 *The effects of environmental factors on chl*-a

Tang *et al*. (2006c) found an inverse relationship between SST and chl-*a* in the sea surface of the Indian Ocean during the 2004 tsunami. The spatial modelling of this study (table 4) allows us to quantify the effect of SST and shows it has a significant negative influence on chl-*a*, except in Week 5, immediately after the tsunami week. The results indicate that the tsunami event might have reduced the negative effect of SST on chl-*a*. The NWR has a significant positive effect on chl-*a* both after and before the tsunami. This is the only relationship that was unaffected by the tsunami. RAF has a notably negative influence on chl-*a*, except in Week 7. WIN has a significant positive effect on chl-*a* before the tsunami, but this effect disappeared after the

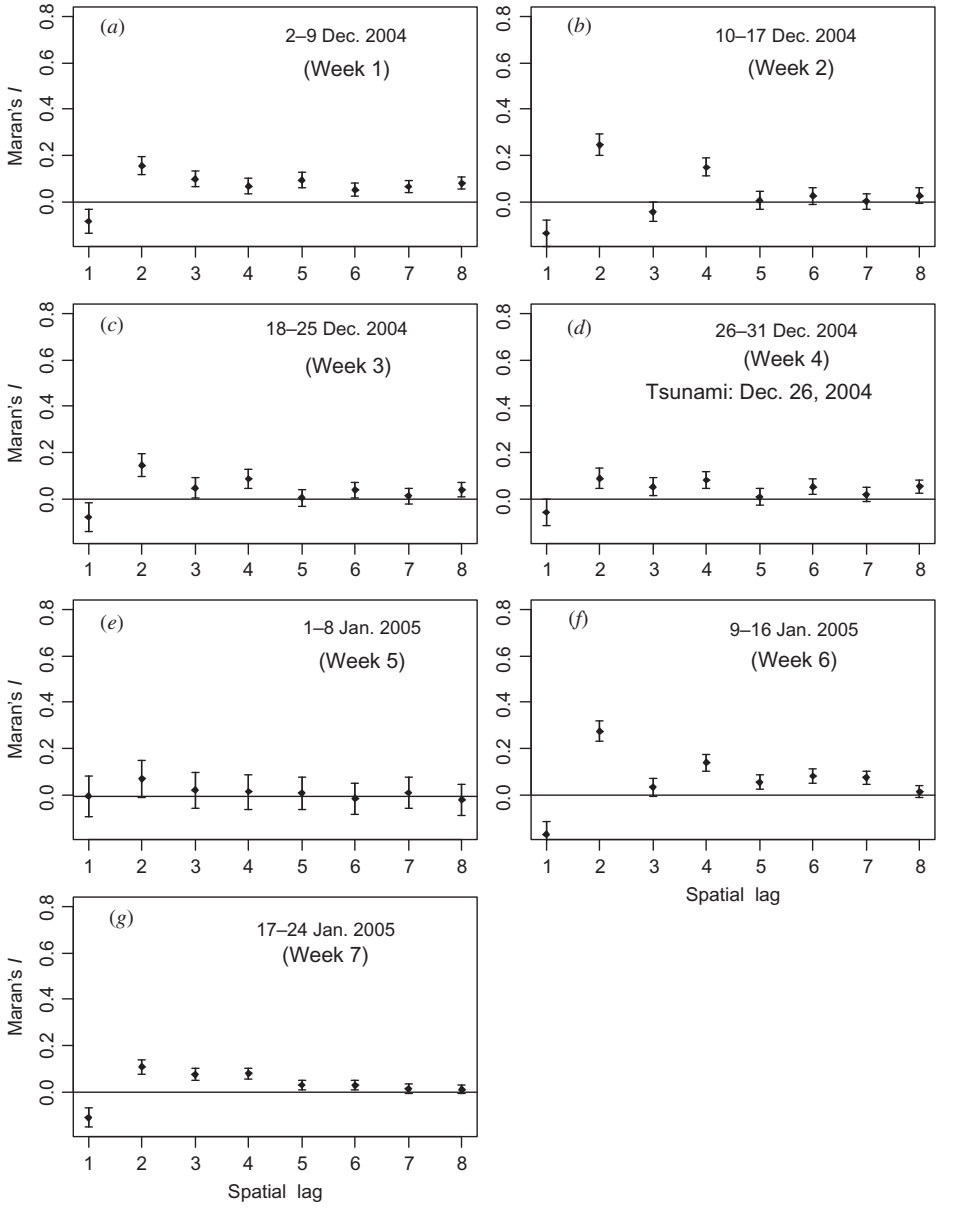

Figure 4. Spatial correlograms for SEM residuals. One spatial lag is 0.5°. The *x*-axis is the number of spatial lags; the *y*-axis is the Moran's *I* value of SEM residuals.

tsunami (Weeks 5, 6). More interestingly, the importance of RAF and WIN to chl-*a* appeared alternately, from Weeks 5 to 7 (table 4). This may be caused by the counteractive effects of RAF (negative) and WIN (positive) on chl-*a*. Except for NWR, the variables SST, WIN and RAF all showed some degree of weakened effect on chl-*a* after the tsunami. This may suggest that the tsunami affects the distributions of chl-*a* and other variables.

Downloaded By: [Zhang, XinFeng] At: 12:35 6 October 2010

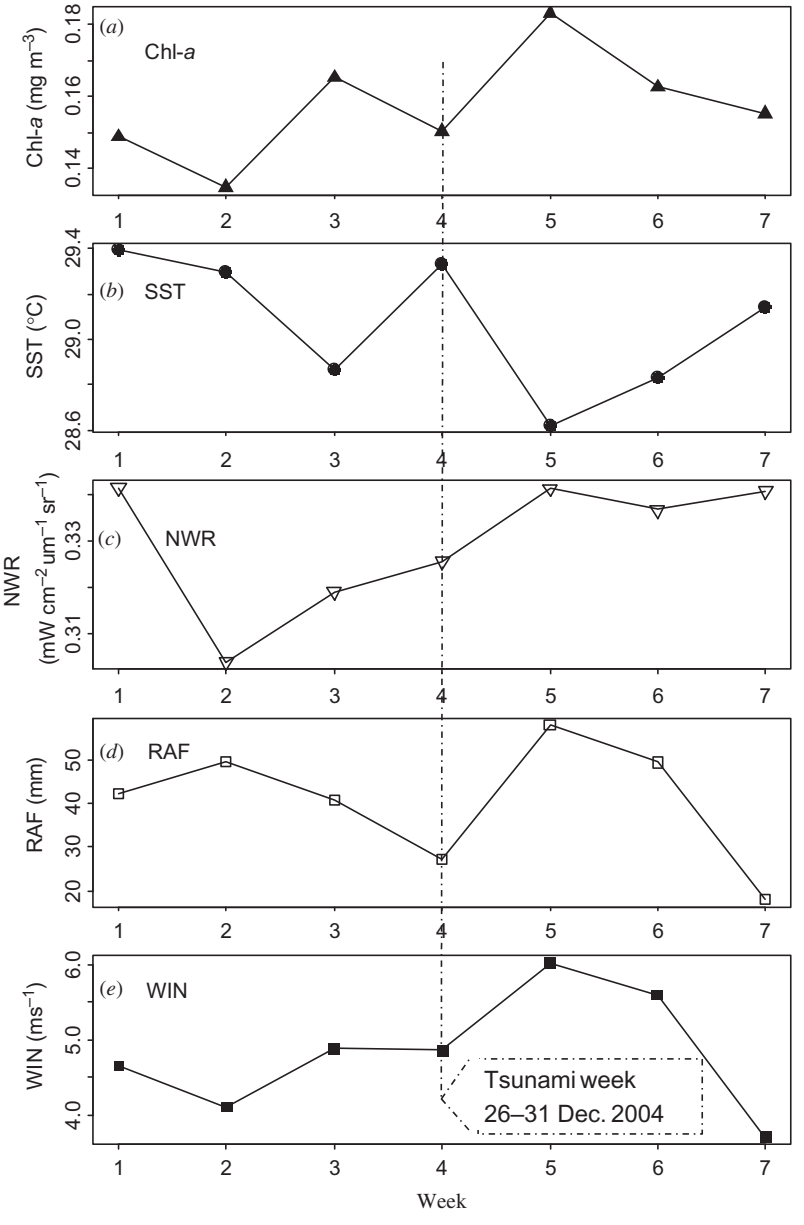

Figure 5. Variations in the means of chl-*a* (mg m^{-3}), SST (°C), NWR (mW $cm^{-2}um^{-1}sr^{-1}$), RAF (mm) and WIN (m s^{-1}) for the seven weeks. Weeks 1, 2 . . . 7 are in the order of the seven weeks shown in table 1. Week 4 is the tsunami week (dashed line).

5.3 *Responses of environmental factors to the tsunami*

Around the occurrence of the tsunami, the five marine environmental factors (chl-*a*, SST, NWR, RAF and WIN) varied differently (figure 5). The changing trends in chl-*a*, NWR and WIN were very similar (figure 5(*a*), (*c*), (*e*)). These changes were also reflected by the results (table 4) in which both NWR and WIN have positive effects on

Downloaded By: [Zhang, XinFeng] At: 12:35 6 October 2010

Table 4. Linear regression analysis of the spatial autoregressive models (SEM).

Week		Intercept	SST	NWR	log(RAF+1)	WIN	λ
1	Coefficient	0.50438	–0.01505	0.27536	–0.00760	0.00466	0.66189
2	Coefficient	0.65675	–0.02113	0.30464	–0.00759	0.00717	0.66477
3	Coefficient	0.51527	–0.01558	0.30583	–0.00945	0.00503	0.61610
4	Coefficient	0.45664	–0.01414	0.33992	–0.00933	0.00471	0.67481
5	Coefficient	0.13617*	–0.00063*	0.29925	–0.01935	0.00157*	0.44924
6	Coefficient	0.62140	–0.01945	0.33019	–0.00557	0.00131*	0.67392
7	Coefficient	0.78124	–0.02572	0.32757	–0.00025*	0.00434	0.73123

*P-value > 0.05
P-value < 0.001 for others (no asterisk). Weeks 1, 2 . . . 7 are in the order of the seven weeks shown in table 1. Week 4 is the tsunami week.

chl-*a*. The variation of chl-*a* before 8 January is consistent with the observation of Singh *et al*. (2007). Tang *et al*. (2006c) found an increase in chl-*a* level along the east coast of India and around Sri Lanka prior to the tsunami. In the present study, the mean of chl-*a* in the whole study area reached its maximum value (0.1833 mg m^{-3}) in Week 5, immediately after the tsunami week (figure 5(*a*)). SST reached its minimum value (28.6°C) in Week 5, immediately after the tsunami week (figure 5(*b*)). At the same time, RAF and WIN increased significantly and reached their maximum values (RAF 57.86 mm and WIN 6.03 m s^{-1}) in Week 5 (figure 5(*d*), (*e*)). The considerable increase in RAF and WIN in Week 5 may be responsible for the significant decrease in SST in the same week. The tsunami event might have played an important role in the sudden changes of marine climate (SST, RAF and WIN) immediately after the tsunami, which might have markedly disturbed the variations in chl-*a*.

6. Conclusions

Our analyses showed that there was a strong spatial and temporal correlation in the distribution of chl-*a*. The tsunami might have caused the fluctuation of spatial autocorrelation in the distributions of chl-*a*. The significant increase in spatial correlation distance in chl-*a*, before the tsunami event, indicated an enhancement in the flow of sea water among neighbouring locations (or grids). The spatial error model revealed that SST and RAF had negative effects on chl-*a*, while NWR and WIN had positive effects. The effects of all the four variables were significant (positive or negative) before the occurrence of the tsunami. It is also clear that, except NWR, the effects of SST, WIN and RAF on chl-*a* disappeared or weakened immediately after the tsunami. There were sudden changes in the marine climate (SST, RAF and WIN) immediately after the 2004 South Asian tsunami, which would have markedly disturbed the distribution of chl-*a*.

The spatial models and the procedure of model estimation used in this study should be of wide application to model other ecological processes in both marine and terrestrial systems as ecological data are often spatially correlated.

Acknowledgements
This study was supported by (1) the National Natural Science Foundation of China (40576053, 40976091 and 40811140533), (2) Chinese Academy of Sciences and the South China Sea Institute of Oceanology (LYQY200701, kzcx2-yw-226), (3) The

Downloaded By: [Zhang, XinFeng] At: 12:35 6 October 2010

CAS/SAFEA International Partnership Program for Creative Research Teams (KZCX2-YW-T001). X.F. Zhang was supported by the China Scholarship Council. The authors thank those professors who have made a contribution to this study.

References

AGARWAL, V.K., MATHUR, A., SHARMA, R., AGARWAL, N. and PAREKH A., 2007, A study of air–sea interaction following the tsunami of 26 December 2004 in the eastern Indian Ocean. *International Journal of Remote Sensing*, **28**, pp. 3113–3119.

ANSELIN, L., 1988, *Spatial Econometrics: Methods and Models*, pp. 16–21, 58–59, 61–72 (Dordrecht: Kluwer).

ANSELIN, L., BERA, A.K., FLORAX, R. and YOON, M.J., 1996, Simple diagnostic tests for spatial dependence. *Regional Science and Urban Economics*, **26**, pp. 77–104.

ANSELIN, L. and FLORAX, R.J.G.M., 1995, *New Directions in Spatial Econometrics*, pp. 25–49 (Berlin: Springer).

ANSELIN, L. and REY, S., 1991, Properties of tests for spatial dependence in linear regression models. *Geographical Analysis*, **23**, pp. 112–131.

BORCADRD, D. and LEGENDRE, P., 2002, All-scale spatial analysis of ecological data by means of principal coordinates of neighbour matrices. *Ecological Modeling*, **153**, pp. 51–68.

CLIFF. A.D. and ORD, J.K., 1981, *Spatial Process: Models and Applications*, pp. 46–51 (London: Pion).

DEY, S., SARKAR, S. and SINGH, R.P., 2004, Anomalous changes in column water vapor after Gujarat earthquake. *Advances in Space Research*, **33**, pp. 274–278.

DEY, S. and SINGH R.P., 2003, Surface latent heat flux as an earthquake precursor. *Natural Hazards and Earth System Sciences*, **3**, pp. 749–755.

GRIFFITH, D.A., 1987, *Spatial Autocorrelation: A Primer*, pp. 9–12 (Washington: Association of American Geographers).

KEITT, T.H., BJORNSTAD, O.N., DIXON, P.M. and CITRON-POUSTY, S., 2002, Accounting for spatial pattern when modeling organism environment interactions. *Ecography*, **25**, pp. 616–625.

KRISHNAKUTTY, N., 2006, Effects of 2004 tsunami on marine ecosystems – a perspective from the concept of disturbance. *Current Science*, **90**, pp. 772–773.

LIU, P.L.F., LYNETT, P., FERNANDO, H., JAFFE, B.E., FRITZ, H., HIGMAN, B., MORTON, R., GOFF, J. and SYNOLAKIS, C., 2005, Observations by the International Tsunami Survey Team in Sri Lanka. *Science*, **308**, p. 1595.

MARTIN, S., 2004, *An Introduction to Ocean Remote Sensing*, pp. 124–165 (Cambridge: Cambridge University Press).

ODLAND, J., 1987, *Spatial Autocorrelation* (Newbury Park, CA.: Sage).

SINGH, R.P., CERVONE, G., KAFATOS, M., PRASAD, A.K., SAHOO, A.K., SUN, D., TANG, D.L. and YANG, R., 2007, Multi-sensor studies of Sumatra earthquake and tsunami of 26 December 2004. *International Journal of Remote Sensing*, **28**, pp. 2885–2896.

SOUSA, W.P., 1979, Disturbance in marine intertidal boulder fields: The nonequilibrium maintenance of species diversity. *Ecology*, **60**, pp. 1225–1239.

STEIN, S. and OKAL, E.A., 2005, Speed and size of the Sumatra earthquake. *Nature*, **434**, pp. 581–582.

TAN, C.K., ISHIZAKA, J., MANDA, A., SISWANTO, E. and TRIPATHY, S.C., 2007, Assessing post-tsunami effects on ocean colour at eastern Indian Ocean using MODIS Aqua satellite. *International Journal of Remote Sensing*, **28**, pp. 3055–3069.

TANG, D.L., KAWAMURA, H., DIEN, T.V. and LEE, M.A., 2004, Offshore phytoplankton biomass increase and its oceanographic causes in the South China Sea. *Marine Ecological Progress Series*, **268**, pp. 31–41.

Downloaded By: [Zhang, XinFeng] At: 12:35 6 October 2010

TANG, D.L., KAWAMURA, H., OH, I.S. and BAKER, J., 2006a, Satellite evidence of harmful algal blooms and related oceanographic features in the Bohai Sea during autumn 1998. *Advance in Space Research*, **37**, pp. 681–689.

TANG, D.L., KAWAMURA, H., SHI, P., TAKAHASHI, W., GUAN, L., SHIMADA, T., SAKAIDA, F. and ISOGUCHI, O., 2006b, Seasonal phytoplankton blooms associated with monsoonal influences and coastal environments in the sea areas either side of the Indochina Peninsula. *Journal of Geophysical Research*, **111**, G01010.

TANG, D.L., SATYANARAYANA, B., ZHAO, H. and SINGH, R.P., 2006c, A preliminary analysis of the Sumatran tsunami influence on Indian Ocean CHL-a and SST. *Advances in Geosciences*, **5**, pp. 15–20.

TANG, D.L., ZHAO, H., SATYANARAYANA, B., ZHENG, G.M., SINGH, R.P. and LV, J.H., 2009, Enhancement of chlorophyll-a in the northeastern Indian Ocean after the 2004 South Asian tsunami. *International Journal of Remote Sensing*, **30**, pp. 4553–4565.

UNEP, 2005, *After the Tsunami: Rapid Environmental Assessment* (Nairobi: United Nations Environment Programme).

WALLER, L.A. and GOTWAY, C.A., 2004, *Applied Spatial Statistics for Public Health Data* (New Jersey: Wiley & Sons, Hoboken).

YAN, Z.Z. and TANG, D.L., 2008, Changes in suspended sediments associated with 2004 Indian Ocean tsunami. *Advance in Space Research*, **43**, pp. 89–95.

ZHANG, X.F., TANG, D.L., LI, Z.Z. and ZHANG, F.P., 2009, The effects of wind and rainfall on suspended sediment concentration related to the 2004 Indian Ocean tsunami. *Marine Pollution Bulletin*, **58**, pp. 1367–1373.

Downloaded By: [Zhang, XinFeng] At: 12:35 6 October 2010